

Morphing the CMB: a technique for interpolating power spectra

Kris Sigurdson¹,

Department of Physics, Simon Fraser University, Burnaby, BC V5A 1S6, Canada

Douglas Scott^{2,3}

*Department of Physics and Astronomy, University of British Columbia,
Vancouver, BC V6T 1Z1, Canada*

Abstract

The confrontation of the Cosmic Microwave Background (CMB) theoretical angular power spectrum with available data often requires the calculation of large numbers of power spectra. The standard practice is to use a fast code to compute the CMB power spectra over some large parameter space, in order to estimate likelihoods and constrain these parameters. But as the dimensionality of the space under study increases, then even with relatively fast anisotropy codes, the computation can become prohibitive. This paper describes the employment of a ‘morphing’ strategy to interpolate new power spectra based on previously calculated ones. We simply present the basic idea here, and illustrate with a few examples; optimization of interpolation schemes will depend on the specific application. In addition to facilitating the exploration of large parameter spaces, this morphing technique may be helpful for Fisher matrix calculations involving derivatives.

Key words: cosmic microwave background, cosmology: theory, methods: numerical
PACS: 98.80-k, 98.70.Vc, 95.75.Pq, 02.60.Ed

1 Introduction

Detailed measurement of the anisotropies on the Cosmic Microwave Background (CMB) sky promises to reveal a wealth of information about the

¹ ksigurds@sfu.ca

² dscott@astro.ubc.ca

³ Corresponding author

Universe in which we live. Spurred on by the rapid advances in CMB experimentation and the promise of the *MAP* (<http://map.gsfc.nasa.gov>) and *Planck* (<http://astro.estec.esa.nl/SA-general/Projects/Planck/>) satellites, there has also been great activity in recent years focussed on CMB theory and data analysis (e.g. Bond 1997). Because of the enormous size of future data sets, anything which might speed up the task of extracting the full cosmological information could be extremely useful.

The power spectrum of CMB anisotropies is usually expressed in terms of the multipole moments C_ℓ , which are the expectation values of the squares in a spherical harmonic expansion of temperatures on the sky. Here ℓ is an inverse angle, and then C_ℓ vs ℓ is just a plot of the power spectrum of fluctuations, analogous to $P(k)$ vs k for a power spectrum derived from Fourier modes in flat space. It is conventional to plot $\ell(\ell+1)C_\ell$ (which is the power per decade in ℓ , and which we will refer to as \mathcal{C}_ℓ) vs ℓ , analogous to $k^2P(k)$ vs k for a flat sky. For a given set of cosmological parameters, the theoretical prediction for the \mathcal{C}_ℓ curve can be calculated quite precisely (see e.g. Hu et al. 1995). For all popular cosmologies one finds a series of bumps and wiggles. It is this rich structure which promises to reveal the values of the cosmological parameters, and which also allows us to utilize the interpolation method described below.

When data from the *COBE* satellite first became available (Smoot 1992) there were a large number of attempts to fit to cosmological models. But the restricted range of angles probed by the *COBE* beam meant that the data were really only sensitive to an amplitude and slope, with some mild constraint on the curvature (Bunn & White 1997). Therefore the suite of models which needed to be considered was relatively modest. As more data from smaller scales became available, probing the acoustic peak region, there were early attempts to constrain a broader range of models (e.g. Scott & White 1995, Bond 1997). As even more data poured in it soon became clear that it was necessary to search a parameter space with a significant number of dimensions (e.g. Hancock et al. 1998, Lineweaver 1998, Bond et al. 1998, Tegmark 1999, Efstathiou et al. 1999, Dodelson & Knox 1999). Some of these studies have attempted to fit likelihoods for models calculated in as many as 6 separate parameter dimensions (or even more using relations between parameters, or other tricks to reduce the dimensionality).

Even larger, and higher quality data sets are expected in future. Long-duration balloon flights such as BOOMERANG are already producing data, and at least three dedicated interferometers are under development. The *MAP* satellite is due for launch in 2000, and the *Planck* mission is due for launch in 2007. Such data sets will require significantly more thorough exploration of the available parameter space in order to extract the most accurate information about our Universe. In practice this will involve the calculation of truly vast databases of theoretical models. As a result, methods of rapidly obtaining the power

spectra are crucial. Codes have been developed (the most widely used being `cmbfast`, Seljak & Zaldarriaga 1996) which efficiently and accurately calculate the anisotropy power spectra. Nevertheless these codes still take a significant amount of time when one considers that there may be a roughly 10 dimensional parameter space to explore. Therefore it is worth considering whether there are any short-cuts which can be taken, with minimal loss of accuracy, for exploring the full parameter space. Some form of accurate interpolation would be particularly useful, since it is orders of magnitude faster to interpolate existing curves than to generate new ones.

The CMB power spectra curves are quite smooth, and vary smoothly with individual parameters, suggesting that it may be unnecessary to perform explicit calculations for every value of a particular parameter – for a reasonable level of accuracy, some type of interpolation is probably sufficient.

The obvious interpolation scheme is simple linear interpolation in the vertical direction. However, given that the curves contain a handful of special features which deform quite smoothly, we can easily imagine interpolation schemes which more explicitly involve continuous changes of one curve into another. Inspired by an idea from image manipulation, sometimes called ‘morphing’,⁴ we explore the use of such an approach for interpolation of CMB power spectra. We are aware of at least one other application of similar ideas in astrophysics, and that is in the generation of stellar isochrones from a relatively small number of stellar mass models, as first applied by Prather (1976), and described in detail by Bergbusch & Vandenberg (1992).

2 Description

The underlying method behind any type of morphing scheme involves selecting certain special features of the images being morphed, defining how these features will be mapped into each other, and then using these mappings to create smooth transformations between the other parts of the objects (see e.g. Wolberg 1990, Magnenat-Thalmann & Thalmann 1990, Gomes et al. 1999). Morphing is just the computerized version of a process which is historically well-known in cinematic animation, where a set of ‘key frames’ is generated by skilled artists, and then the process of ‘in-betweening’, or filling in the steps between these frames is performed by less skilled artists. A common example used to display the effectiveness of morphing in computer graphics is that of

⁴ Definition: ‘The animated transformation of one image into another by gradually distorting the first image so as to move certain chosen points to the position of corresponding points in the second image’ (from the Free On-Line Dictionary of Computing, <http://foldoc.doc.ic.ac.uk>).

two different human faces being morphed into each other, passing continuously through a composite face. In this case the special features might be the eyes, nose, mouth, and cheekbones, and these features might be mapped into each other using linear interpolation along a straight line between corresponding points of the picture. A smooth mapping field for the rest of the picture could then be generated by interpolating between these mapping vectors.

The procedure is very much the same when morphing is used to smoothly interpolate between two similar curves. The difference in this case is that usually each curve is associated with a vector of parameters, and we wish to accurately interpolate the intermediate curve associated with some intermediate parameter vector (corresponding to ‘tweening’ in animation). Analogous to the eyes or nose of a face, physically or mathematically significant points on the curve are chosen to be the special features which are mapped into each other – these are known as the morphing ‘control points’. The locations of these control points on the intermediate curve – which we call ‘target points’ – is interpolated using the control points from the original curves and the associated parameter vectors. Once the locations of these target points has been determined, a vector is constructed between each control point and the corresponding target point. By interpolating between these vectors a mapping field is created that will morph the curves to the shape approximating the curve at any intermediate location in the parameter space.

Having understood the general principle, the question is: can the CMB angular power spectrum be interpolated using some type of morphing algorithm? The fact that it changes smoothly and continuously as cosmological parameters are varied suggests that the answer is ‘yes’. We give some examples to illustrate this below.

At this point it is worth stressing why this morphing approach is superior to linear interpolation. The basic reason is that morphing involves interpolating the curves *in a coordinate system which is matched to the physical process* which is distorting the curves. A good analogy is to consider how to interpolate between two circles of different radii. To make the problem single-valued, consider only the semi-circles with positive y -coordinate. Now imagine trying to interpolate to another semi-circle with an intermediate radius. It is obvious that linear interpolation in the vertical coordinate is hopeless, and that switching to polar, and interpolating radially, is the sensible approach. The point about morphing, using special points on the curves, is that one is effectively using the coordinate system in which the curves are naturally changing. So once we interpolate the curves in this ‘morphological coordinate system’, then we can perform interpolation in the usual way, except that we have now used the shape information of the curves to define the direction in which to interpolate.

3 Details

We now describe each step in the morphing procedure. We will assume that a set of curves covering the range of parameters of interest has already been calculated, and we are attempting to interpolate a ‘target curve’ at some intermediate parameter value (see Fig. 1).

Note that for many of these steps several different choices could be made. In no case do we claim that what we describe below represents the optimal choice. Rather, we hope that our outline of the algorithm is detailed and clear enough to stimulate other studies.

3.1 Choose control points

The first step in any morphing process is to choose which points will be used as the morphing ‘control points’. Morphing control points are special points on the curves defining the path through which morphing occurs as a function of the interpolation parameter.

It is helpful conceptually to separate the control points into two classes, primary control points and secondary control points. Primary control points are easily identifiable features on the curves, and track gross changes in the shape of the curve, while secondary control points are selected between the primary points and track the higher order effects. The criteria for good primary control points are that they are morphologically significant, and easy to determine automatically.

The obvious choice for the primary control points for the CMB power spectra are the maxima and minima, which are also significant in that they are related to the underlying physical processes. Because the CMB power spectrum is relatively simple and smooth, a good choice for the secondary control points might be the inflection points of the curve, i.e. the extrema of the derivatives. However, once the primary control points have been selected, there are many options for secondary control points, because they are only tracking small deviations in the shape of the curve. Another class of points are those which lie some definite fraction of the way vertically (or horizontally) between a maximum and a minimum. One advantage of these points is that they are unambiguously unique, owing to their construction between a maximum and a minimum. We have found that these points may be a better choice for secondary control points, since inflection points or the extrema of higher order derivatives are numerically difficult to find with sufficient accuracy. In the examples which follow, we have used as secondary points those points $1/4$, $1/2$ and $3/4$ of the vertical distance between the primary points.

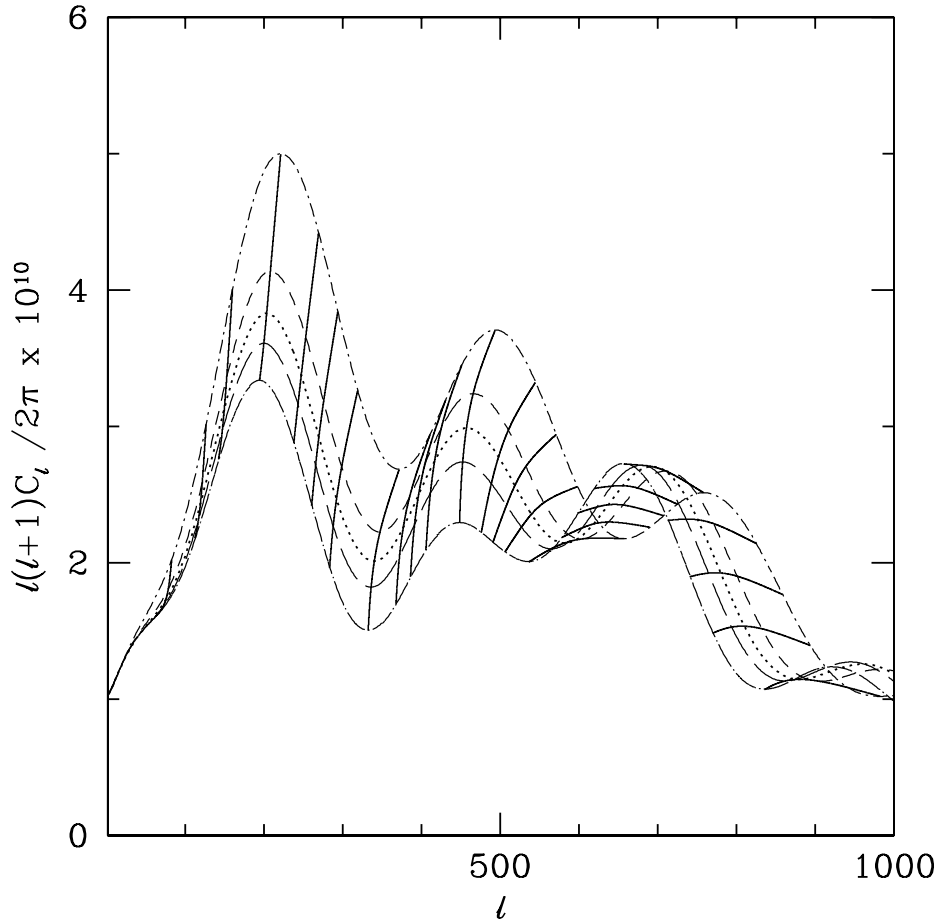


Fig. 1. This figure shows how 4 point cubic splines can be used interpolate the target points for CMB anisotropy power spectra. Dashed and dot-dash lines represent 4 different cosmological models (actually different values of the Hubble constant). For definiteness we chose standard Cold Dark Matter type models, and concentrated on multipoles $\ell = 2$ –1000. The solid lines indicate spline fits to the positions of primary and secondary control points. The dotted line shows the interpolated model.

There is also a question of what to use as control points at the lowest and highest multipoles considered. In our examples we simply chose $\ell = 2$ and $\ell = 1500$ as control points, which is certainly not optimal – it would be better to choose something more physical than just the end-points. In practice, however, it is less important to be fully accurate at the lowest ℓ s, where cosmic variance is large, and at the very highest ℓ s, where the primordial spectrum falls off.

3.2 Find control points

Once the control points have been selected they must be extracted from each curve. For the purposes of morphing it is useful to consider the CMB power spectrum as a continuous function of ℓ , for which we only have samples at integer ℓ . Using standard routines it is straightforward to determine the maxima and minima of this function. Finding secondary control points based on these maxima and minima is equally straightforward. If we wanted instead to determine the inflection points of this function, a derivative would need to be calculated at this stage. Precautions must be taken to ensure the original functions are free of high frequency noise prior to this step, as unwanted inflection points induced by noise introduce an ambiguity that can play havoc when mapping the control points. In practice we low-pass filtered when we examined numerical differences – but even so – we found that it was difficult to accurately pin down turning points in the derivatives of the \mathcal{C}_ℓ s.

3.3 Calculate the target points

The next part of the procedure involves finding the points on the intermediate curve which correspond to the control points – we call these the ‘target points’.

In fact the key step that governs how accurately an intermediate set of \mathcal{C}_ℓ s can be determined is how accurately the target points can be interpolated from the control points. The simplest method would be to linearly interpolate between sets of control points on two existing curves. The next simplest method would be to use the curves from several points in parameter space instead of just two, and to use spline interpolation to obtain the target points from the sets of control points. Although the lowest-order cubic spline requires more (actually 4) sets of \mathcal{C}_ℓ s compared with linear interpolation, the accuracy of the method is significantly improved (as described later). We therefore adopted 4 point cubic spline interpolation to find the target points in the morphing studies described here.

3.4 Map control points

From the point of view of writing a code to automate the morphing process, the thorniest step is mapping one set of control points into another set. The morphology of each \mathcal{C}_ℓ curve can be classified based on the set of primary control points extracted from it. Even though the CMB power spectrum smoothly and continuously changes shape, the morphology can and does change *discontinuously* at some parameter values. There are two major ways that the

morphology can change from one set of parameters to another. The first is an artifact of simulating the power spectrum over a finite range of ℓ s, and occurs when a minimum or maximum enters or leaves the edge of the simulated range. The second reflects an actual change in the morphology of the curve, and occurs when a maximum and minimum simultaneously disappear or appear on the curve at some intermediate location. The tricky part of mapping control points is detecting which combination of morphological changes has occurred, and then mapping the control points accordingly. Each \mathcal{C}_ℓ curve could also be classified at a more detailed level based on the secondary control points if they have some non-uniform structure, however this would further complicate the mapping algorithm.

Successfully mapped control points are used to generate the target points for the warping stage. Although a change in morphology will leave some control points unmapped – and thus unwrapped – the final step in the process will interpolate these regions accurately.

Exactly how versatile this mapping process needs to be obviously depends strongly on the parameter range being explored. In practice one could calculate in advance the places in parameter space where maxima and minima converge, and be prepared for this. Ultimately this may not even work, and for some parameter ranges, it may be necessary for the interpolation algorithm simply to instruct the user to provide further \mathcal{C}_ℓ curves in order for accurate interpolation to be achievable.

3.5 Warp curves

After the control points have been mapped, and the target points generated, each of the curves nearest to the desired location in parameter space are ‘warped’ into the expected shape. A nice way to envision the warping is to separate it into two steps. First, the curve is re-parameterized on the horizontal axis to a coordinate system where the control points are aligned vertically at the target ℓ value. Secondly, the curves are then cubic spline interpolated in the vertical direction, constraining the warped curve to pass through the target points.

In practice it may be easier to consider each \mathcal{C}_ℓ curve to be a vector function \vec{f} . From this point of view, at the k th control point a warp-vector is created that will move the control point into the target point, i.e.

$$\vec{f}_k \equiv [\Delta\ell_k, \Delta(\mathcal{C}_\ell)_k], \quad (1)$$

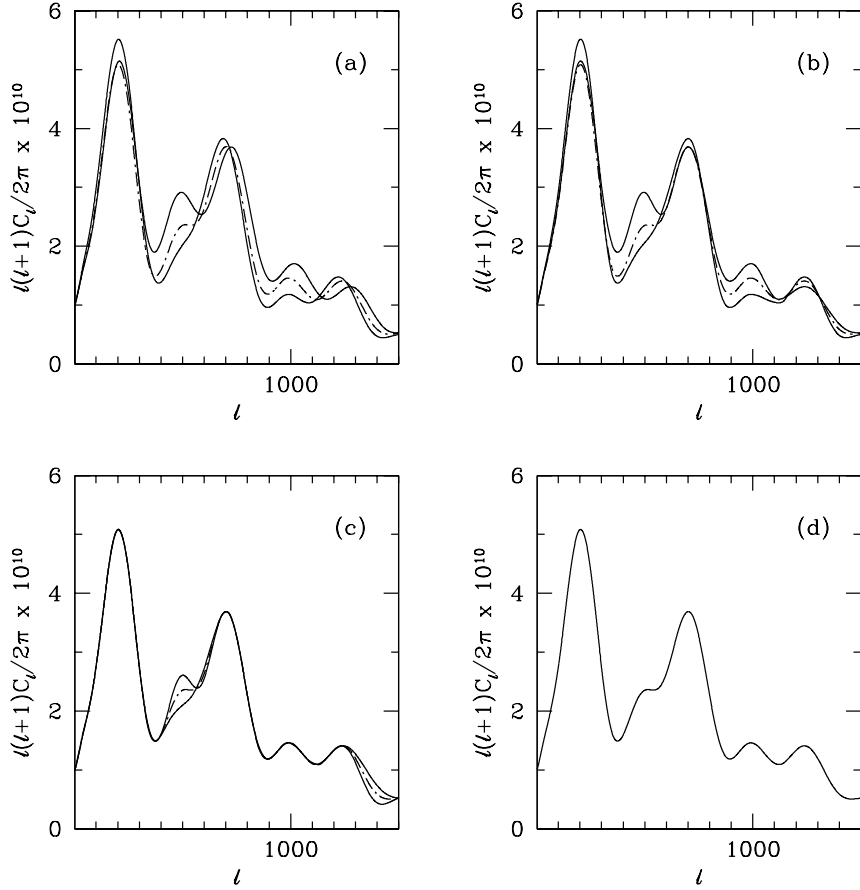


Fig. 2. Demonstration of the method with three sets of computed C_ℓ s, one at a parameter value intermediate to the other two (dot-dash curve): (a) starting point; (b) after horizontal warping; (c) after vertical warping as well; (d) after weighted averaging of the two warped curves. In the final panel the interpolated (solid) curve covers the target (dot-dashed) curve almost exactly.

where

$$\Delta \ell_k \equiv \ell_k^{\text{target}} - \ell_k, \quad (2)$$

and

$$\Delta (\mathcal{C}_\ell)_k \equiv (\mathcal{C}_\ell)_k^{\text{target}} - (\mathcal{C}_\ell)_k. \quad (3)$$

A spline is used to interpolate between these vectors, generating a smooth warp-vector function $\Delta \vec{f}$. By applying this type of function to both of the

nearby \mathcal{C}_ℓ curves, two warped curves are generated, $(\mathcal{C}_\ell^1)'$ and $(\mathcal{C}_\ell^2)'$, that approximate the curve at the desired location in parameter space:

$$\vec{f} \longrightarrow \vec{f}' = \vec{f} + \Delta\vec{f}, \quad (4)$$

$$[\ell, (\mathcal{C}_\ell)] \longrightarrow [\ell', (\mathcal{C}_\ell)'] = [\ell + \Delta\ell, (\mathcal{C}_\ell) + \Delta(\mathcal{C}_\ell)]. \quad (5)$$

3.6 Obtain the final curve

The penultimate step in the process is to re-grid the warped \mathcal{C}_ℓ curves onto integer values of ℓ again, and calculate the weighted average of the two warped curves at each ℓ , i.e.

$$(\mathcal{C}_\ell)^{\text{target}} = x(\mathcal{C}_\ell^1)' + (1 - x)(\mathcal{C}_\ell^2)', \quad (6)$$

where $0 < x < 1$. For example if we are interpolating the curve at a parameter value exactly half-way between the value at the two curves, then $x = 1/2$ and we have the simple average of the warped curves. This final step ensures that the transition between curves will be continuous, and will complete the morphing process in regions near morphological discontinuities. A step-by-step pictorial summary of the morphing process is shown in Fig. 2.

4 Accuracy

There are various places where the details of our approach are probably not optimal, and where further study could be done. For all subsections of Section 3 there are possible refinements which might improve the accuracy. Examples include: choice of primary control points and number of secondary control points; numerical method of finding these points; interpolation procedure for obtaining the target points, including the number of curves used and the method of interpolating between them; the detailed procedure for interpolating between the warp-vectors; and the method of weighting the two warped curves to obtain the target curve. The best method may depend on details of the problem being addressed, e.g. the parameter range, value of ℓ_{max} etc. Indeed, even the statistic for describing how well the interpolation has performed might depend on the specific application. For example, should the error be weighted by the inverse of the cosmic variance?

There are several statistics that we felt might be relevant when considering the accuracy of this method, including maximum error, location of maximum error, average error, and error in the total power ($\sum(2\ell+1)\Delta\mathcal{C}_\ell$). These statistics

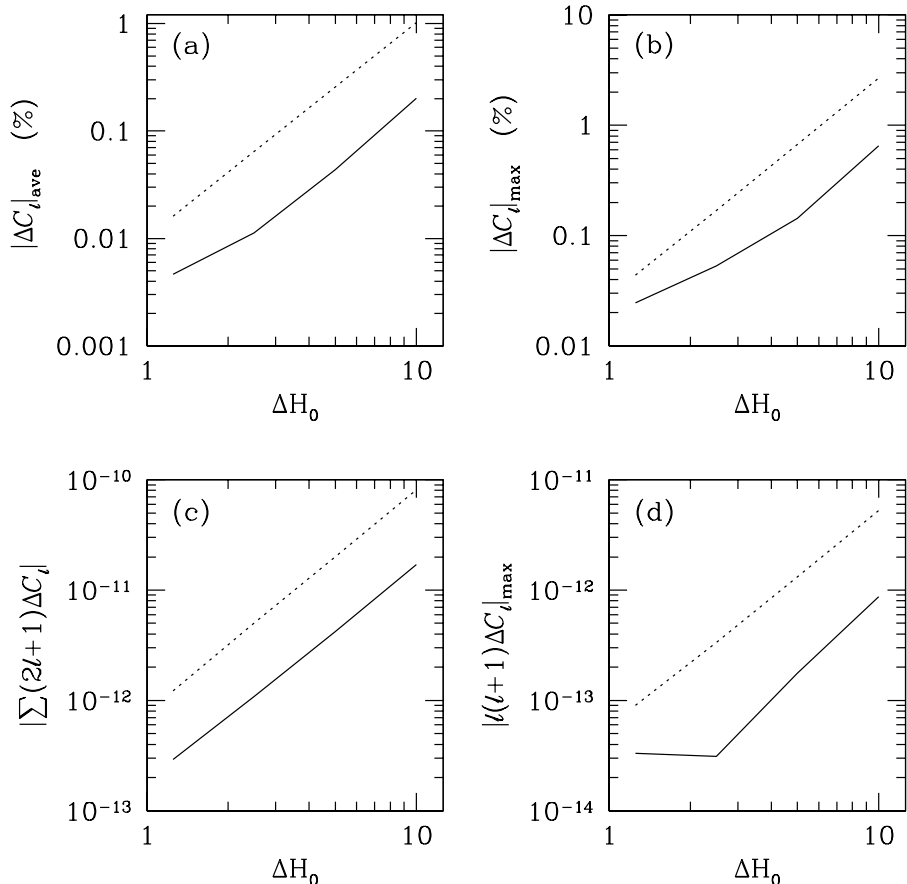


Fig. 3. Quantification of error for one example of morphing interpolation, in the Hubble constant, shown as a function of the grid spacing in H_0 : (a) mean percentage error; (b) maximum percentage error; (c) deviation in total power; (d) maximum absolute deviation. The dotted line represents linear interpolation, while the solid line is for morphing.

(actually their absolute values) are plotted for several cases in Fig. 3. Another possibility is to consider the deviation in the cummulants of the curves, i.e.

$$\max \left\{ \sum_{\ell=2}^k (C_\ell^1 - C_\ell^2) \right\}, \quad (7)$$

which gives similar results.

Fig. 3 is for the specific example of interpolation in H_0 , around the parameter values of the standard Cold Dark Matter model. We see that morphing reduces the maximum percentage error, average percentage error, total power

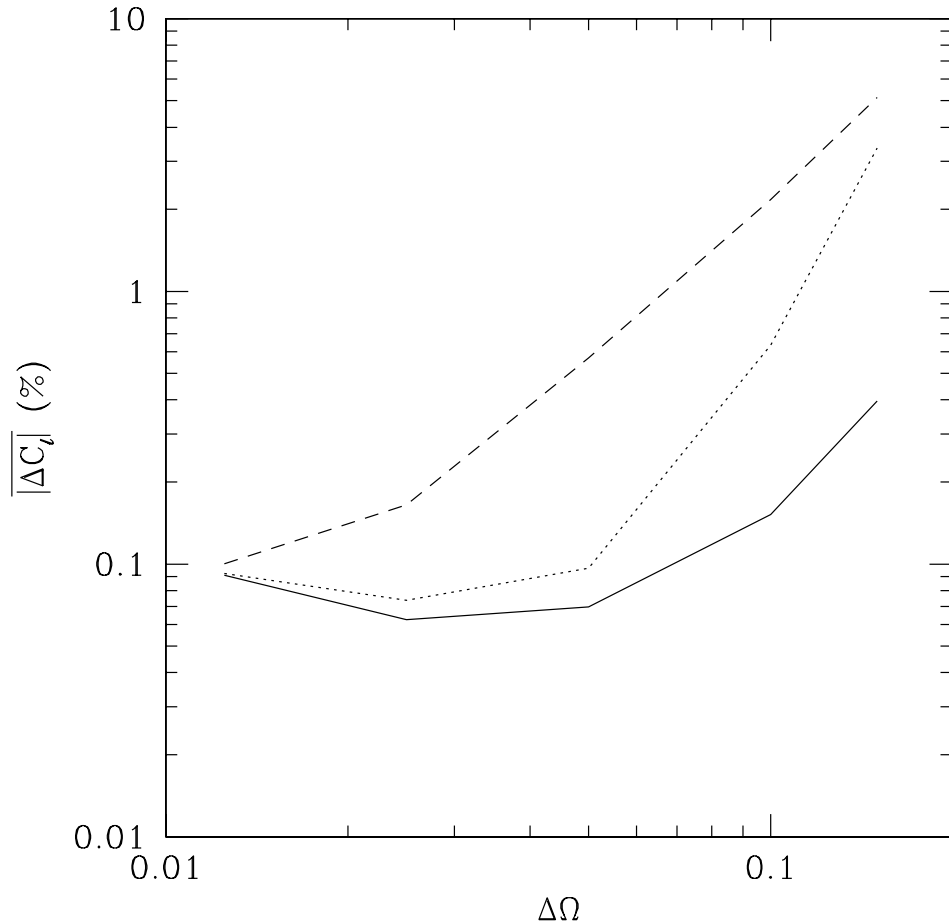


Fig. 4. Mean percentage error as a function of the grid spacing in Ω_0 . The dashed line shows linear interpolation, while the dotted line shows cubic spline interpolation in the vertical direction, and the solid line is for morphing.

error, and the maximum absolute error all by a factor ~ 5 over vertical linear interpolation. Note that as the grid spacing is reduced the error functions start to converge, due to the noise limitations of specific runs of the `cmbfast` code which we used.

Now let us look at morphing in another parameter. As Ω_0 (the density parameter, assuming here that there is no cosmological constant) is decreased, then to a first approximation the location of the peaks of the power spectra are simply shifted to higher values of ℓ . Because of this, we expect that morphing on Ω_0 should be far superior to vertical interpolation on Ω_0 . Indeed, in Fig. 4 we see that, for large grid spacing, morphing reduces the average absolute percentage error by a factor of ~ 13 compared to vertical linear interpolation. And even if we used cubic spline interpolation in the vertical direction, we find

that morphing is still better by a factor of ~ 8 . Again, as the grid spacing in Ω_0 is reduced all three curves rapidly converge to the level of accuracy with which the model \mathcal{C}_ℓ s were generated. However, if the original \mathcal{C}_ℓ s are calculated more precisely, then morphing continues to give accurate results down to smaller parameter spacing.

In practice morphing will be used on a grid of several parameters at once. Multi-dimensional interpolation is complicated by the fact that the final answer usually depends on the order of the parameters one interpolates with. Therefore, another useful comparison is to perform morphing on two different parameters in the two possible orders, and examine how closely the end results match. This tests the linearity of the method, and gives another estimate of its accuracy. As an example we examine morphing for the baryon fraction Ω_b and the dimensionless Hubble parameter h . For typical grid spacings, Fig. 5 indicates that the maximum deviation between the two possible permutations is on the order of 0.1%, with the average deviation an order of magnitude less.

Interpolation between the models is inherently several orders of magnitude faster than direct calculation. While this algorithm does have several extra steps compared with simple vertical interpolation, the actual runtime for morphing is comparable. It is certainly essentially instantaneous compared to direct calculation of the \mathcal{C}_ℓ s.

5 Discussion

It is clear that vertical interpolation is optimized when the major changes in the shape of the curve occur vertically. The major advantage of morphing over simple vertical linear (or cubic spline) interpolation is the ability to accurately track horizontal distortions of a curve as well. Morphing is particularly useful in regions of the curve where the slope is steep, as these small horizontal shifts in the curve will result in large vertical shifts at a fixed horizontal coordinate. Morphing can track these changes more accurately because when morphing, we effectively change to a coordinate system which tracks the major changes in the shape of the curve – the ‘morphological coordinate system’.

Let us introduce a parameter, λ , which tracks whether the curves are being interpolated vertically in the initial coordinate system, or along vectors suggested by the control points (vertically in the morphological coordinate system) – λ can be any smooth function, such as an angle, describing the interpolation direction. For simplicity we will define $\lambda = 0$ to be simple vertical interpolation, $\lambda = 1$ is the morphing direction, and $\lambda > 1$ is interpolation along vectors which are even more horizontal than that. Explicitly we can take λ to

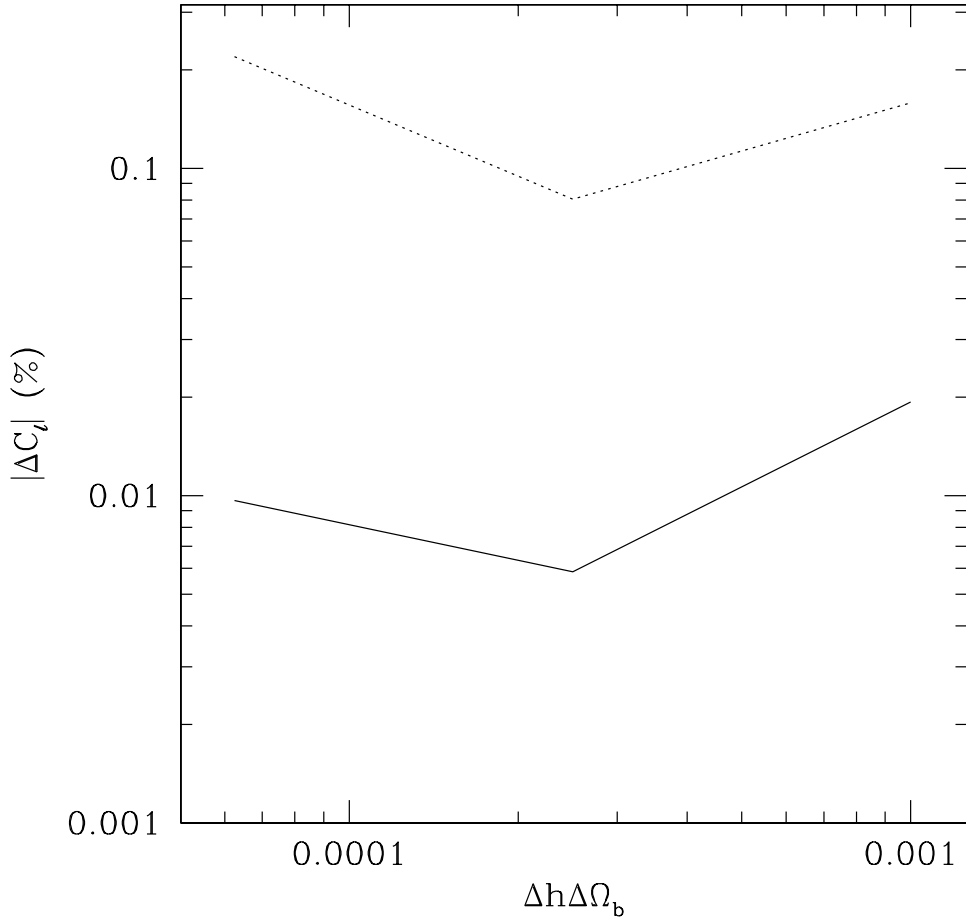


Fig. 5. The difference between the two possible permutations of a two dimensional morph on the parameters h and Ω_b , plotted as a function of the unit grid area. The solid line indicates the average deviation, while the dotted line shows the maximum deviation.

be the fraction of horizontal transformation that we use, i.e. take

$$\ell \rightarrow \ell' = \ell + \lambda \cdot \Delta\ell, \quad (8)$$

where $\Delta\ell = \ell^{\text{target}} - \ell$. A good indicator of the relative accuracy that can be achieved by vertical interpolation between two well behaved curves is their mean normalized absolute difference:

$$\langle \Delta_N \rangle \equiv \left\langle \frac{|f_1 - f_2|}{\min[f_1, f_2]} \right\rangle. \quad (9)$$

A lower value of this statistic indicates that the average normalized vertical

distance between the two curves is less, and consequently the magnitude of the errors induced by vertical interpolation is nearly always reduced.

Fig. 6 shows an example of a calculation of this statistic for a particular CMB power spectrum interpolation. What we see is that as we continuously transform from the original coordinates to the morphological coordinates, Δ_N goes through a minimum near $\lambda = 1$, the value of λ in the morphological coordinate system. This graph indicates that by changing to the morphological coordinate system we expect the errors introduced by vertical interpolation to be reduced. Because the errors introduced by transforming to the morphological coordinate system are relatively small, the overall effect of morphing is to reduce interpolation errors.

The process of morphing keeps track of the most important information about a function from a numerical standpoint. If the locations and values of the maxima and minima of a function and several derivatives are known, we can easily reconstruct a very good approximation to that function. Since often the important physical information we can extract from a curve is encoded in these prominent features of the curve, it makes sense to devote most effort to interpolation of these features. In fact, it may be fruitful to look into the possibility of replacing the thousands of \mathcal{C}_ℓ s with a smaller vector of numbers that keeps track of the prominent features of the curve. If we stop the morphing algorithm after the control points have been determined, we effectively accomplish this ‘compression’ of the critical information in the power spectrum (the advantage of our algorithm is that by smoothly warping the curves we use information from the regions *between* the control points to reduce inaccuracies). One can easily imagine trying to reconstruct the power spectrum using *only* the control points – at the cost of additional inaccuracy. Alternatively, one could attempt to directly fit the positions of the control points as a function of the cosmological parameters. We leave such investigations to future studies.

The most troublesome instabilities in the morphing algorithm arise because of the discrete nature of the power spectrum. Near to morphological discontinuities the algorithm may try to explode a small region around the discontinuity, of say $\Delta\ell \simeq 10$, to cover a much larger span in ℓ . This results in an excessively flat function over this region that dramatically increases the error. The solution to this problem is to create a ‘buffer zone’ around regions of the \mathcal{C}_ℓ curve near morphological discontinuities in parameter space, to prevent points in these regions from being used as control points.

Other improvements are probably possible. We have not explored whether additional physical information, such as known approximate dependencies on parameters in certain regions of the parameter space, would significantly improve the interpolations. For example, we can certainly imagine that using a power law in Ω_K (the curvature) might be a better way of interpolating be-

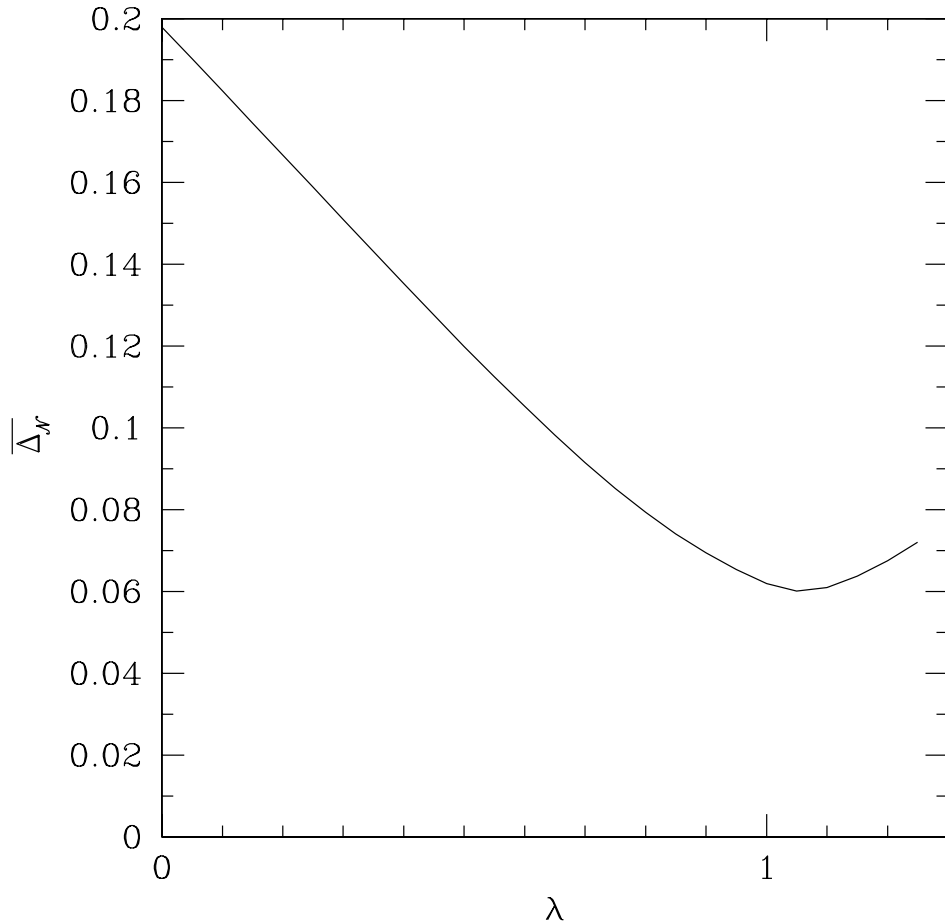


Fig. 6. The mean normalized difference between the nearest interpolating curves is shown as a function λ , a parameter which tracks the transformation to the morphological coordinate system. $\lambda=0$ represents the original coordinate system (i.e. vertical interpolation), $\lambda=1$ represents a full transformation to morphological coordinates (i.e. interpolating along the vector separating the control points), and $\lambda, > 1$ represents an over-transformation (i.e. further from the vertical than even the morphing direction).

tween the control points than the spline fit that we have used. The positions and heights of the peaks can be understood analytically (e.g. Hu, Sugiyama & Silk 1997) through the physics of acoustic modes driven by gravity. Hence it might be possible to replace the spline interpolation step of the morphing algorithm with a function which is more physically motivated. Another refinement might be to include a control point related to the curvature scale at low ℓ in open or closed models (or the angular scale corresponding to the epoch when potentials are decaying in models with a cosmological constant). Further elaborations of morphing will depend on the parameter ranges being

considered.

6 Applications

The most obvious application for morphing is in the construction of large likelihood grids for the analysis of future CMB data sets. If every M th grid point is calculated by direct means, morphing reduces the calculation time by a factor of nearly M^N , where N is the dimensionality of the likelihood space being explored. While this fact is also true for simpler forms of interpolation, the increased accuracy of morphing allows for larger values of M while maintaining the same level of approximation. Techniques like this will be crucial for the searches in ~ 10 parameters that will soon be necessary.

Another possible application of the increased accuracy of morphing is when calculating derivatives of the \mathcal{C}_ℓ s with respect to the model parameters. These derivatives are useful for Fisher matrix studies (e.g. Eisenstein et al. 1999), for instance. Morphed interpolation allows for much smoother and slightly more precise estimates of the derivatives.

7 Conclusions

Morph-interpolation gives a way to confront the problem of exploring large likelihood spaces to a satisfactory degree of accuracy. The superiority of morphing to simple vertical interpolation is apparent. This superiority comes at the cost of a modest increase in coding complexity, but little increase in computation time.

Morphing has recently become an integral part of the modern computer graphics artist's repertoire. We hope that this paper will stimulate interest in morphing as an approach to interpolation, and that it might also encourage people to look for inspiration outside of astrophysics when tackling new problems such as those associated with the confrontation of CMB data with theoretical models.

Acknowledgements

This research was supported by the Natural Sciences and Engineering Research Council of Canada. The code `cmbfast`, developed by Uroš Seljak and Matias Zaldarriaga, was used to generate the \mathcal{C}_ℓ s.

References

- Bergbusch P.A., VandenBerg D.A., 1992, *ApJS*, 81, 163 (1992ApJS...81..163B)
- Bond J.R., 1997, in *The Evolution of the Universe*, Dahlem Workshop Report, ed. G. Borner, S. Gottlöber, J. Wiley, New York, p.199 (1997evun.work...199B)
- Bond J.R., 1997, in *Microwave Background Anisotropies*, Proc. XVIth Moriond Astrophysics Meeting, ed. F.R. Bouchet et al., Editions Frontieres, France (astro-ph/9610119)
- Bond J.R., Jaffe A.H., Knox L.E., 1998, *ApJ*, in press (astro-ph/9808264)
- Bunn E.F., White M., 1997, *ApJ*, 480, 6 (astro-ph/9607060) (1997ApJ...480....6B)
- Dodelson S., Knox L., 1999, *Phys. Rev. Lett.*, submitted (astro-ph/9909454)
- Efstathiou G., Bridle S.L., Lasenby A.N., Hobson M.P., Ellis R.S., 1999, *MNRAS*, 303, L47 (astro-ph/9812226) (1999MNRAS.303L..47E)
- Eisenstein D.J., Hu, W., Tegmark M., 1999, *ApJ*, 518, 2 (astro-ph/9807130) (1999ApJ...518....2E)
- Gomes J., Costa B., Darsa L., Velho L, 1999, *Warping and Morphing of Graphical Objects*, Morgan Kaufmann Series in Computer Graphics and Geometric Modeling, Academic Press, San Francisco
- Hancock S., Rocha G., Lasenby A.N., Gutierrez C.M., 1998, *MNRAS*, 294, L1 (astro-ph/9708254) (1998MNRAS.294L...1H)
- Hu W., Scott D., Sugiyama N., White M., 1995, *Phys. Rev.*, D52, 5498 (astro-ph/9505043) (1995PhRvD..52.5498H)
- Hu W., Sugiyama N., Silk J., 1997, *Nature*, 386, 37 (astro-ph/9604166)
- Lineweaver C.H., 1998, *ApJ*, 505, L69 (astro-ph/9805326) (1998ApJ...505L..69L)
- Magenat-Thalmann N., Thalmann D., 1990, *Computer animation: theory and practice*, Springer-Verlag, New York
- Prather M.J., 1976, Ph.D. thesis, Yale University
- Scott D., White M., 1995, in *CMB Anisotropies Two Years After COBE*, ed. L.M. Krauss, World Scientific, Singapore, p.214 (astro-ph/9407073)
- Seljak U., Zaldarriaga M., 1996, *ApJ*, 469, 437 (1996ApJ...469..437S)
- Smoot G.F., et al., 1992, *ApJ*, 396, L1 (1992ApJ...396L...1S)
- Tegmark M., 1999, *ApJ*, 514, 69 (astro-ph/9809201) (1999ApJ...514L..69T)
- Wolberg G., 1990, *Digital Image Warping*. IEEE Computer Society P., Los Alamitos, CA.